

# Synthesis of nanocrystalline $\text{Ni}_1\text{Co}_{0.2}\text{Mn}_{1.8}\text{O}_4$ powders for NTC thermistor by a gel auto-combustion process

Weimin Wang, Xiangchun Liu, Feng Gao, Changsheng Tian\*

*School of Materials Science and Engineering, Northwestern Polytechnical University,  
Youyi West Road 127, 710072 Xi'an, Shanxi Province, PR China*

Received 19 May 2005; received in revised form 2 September 2005; accepted 27 October 2005

Available online 15 February 2006

## Abstract

Nanocrystalline  $\text{Ni}_1\text{Co}_{0.2}\text{Mn}_{1.8}\text{O}_4$  powders were synthesized via a gel auto-combustion process of nitrate–citrate gels. The investigation on the gels by XRD shows that a stable sol–gel can be formed by adding ethylene glycol (EG) and adjusting the pH values. The dried gels exhibit auto-catalytic combustion behavior. The reaction mechanism has been given by detailed studies based on DTA–DSC and XRD techniques. After being sintered at about 1150 °C, well-densified NTC ceramics with  $B$  values higher than 3600 k were obtained. It is demonstrated that the synthesized powder is high sinter active, and can be used for NTC thermistor application.

© 2006 Elsevier Ltd and Techna Group S.r.l. All rights reserved.

**Keywords:** A. Sol–gel process; B. Nanocomposition; NTC thermistors

## 1. Introduction

Complex spinel oxides based on transition metals such as Co, Ni and Mn are of significant interest, owing to their technology application as negative temperature coefficient (NTC) thermistors for temperature measurement and control. High quality powder of  $\text{NiCoMnO}_4$  is a very important factor to the NTC thermistor. The powders can be synthesized by different methods, which include the traditional solid method; the ethylene glycol–metal nitrate polymerized complex process [1], co-precipitation with different precipitators [2]. It is also well known that the dried nitrate–citrate gels exhibit auto-catalytic combustion behavior and that low-temperature combustion synthesis has been proved to be a simple and economic way to prepare the ultrafine powders [3]. According to current literature, no attempt has been done to synthesize the  $\text{NiCoMnO}_4$  powder via the nitrate–citrate gel auto-combustion process. So, we tried to synthesize the  $\text{NiCoMnO}_4$  powder by this method. The ultrafine powders were obtained and characterized. The powders were used to prepare the NTC ceramics. Especially, the reaction mechanism was studied in this paper.

## 2. Experimental procedure

Analytical grade  $\text{Ni}(\text{NO}_3)_2 \cdot 6\text{H}_2\text{O}$ ,  $\text{Co}(\text{NO}_3)_2 \cdot 6\text{H}_2\text{O}$ ,  $\text{Mn}(\text{NO}_3)_2$  (50%), citric acid, and ethylene glycol (EG) were used as raw materials. According to the composition of  $\text{Ni}_1\text{Co}_{0.2}\text{Mn}_{1.8}\text{O}_4$ , the appropriate amount of nitrates and citric acid were dissolved into de-ionized water to form mixed solutions. Ammonia was dropped into the solutions to change the pH value from 3 to 6. In the end, appropriate amount of EG was added into the solutions. The solutions were heated at 80 °C to form the sol, then were heated at 130 °C under constant stirring to transform into the dried gel. Being ignited in the air at room temperature, as-burnt powders were obtained, then, the as-burnt powders were calcined at 300–800 °C. Ultrafine powders were obtained. Fig. 1 gives the flow chart for preparing  $\text{Ni}_1\text{Co}_{0.2}\text{Mn}_{1.8}\text{O}_4$  powder.

The dried gel precursors were characterized via TG and DSC (NETZSCH STA 449C) at a heating rate of 10 °C/min in static air. The phase identification of the gel precursors, as-burnt powders and as-calcined powders were performed using X-ray diffractometer (X'Pert HighScore) with Cu K $\alpha$  radiation.

The synthesized powder was granulated using PVA as a binder, and uniaxially pressed to form green specimens. After binder burnt-out at 500 °C for 1 h, the specimens were sintered in static air at 1150 °C. Compact bodies could be obtained,

\* Corresponding author. Tel.: +86 29 88492137/13119125257.

E-mail address: wwm0811@sina.com.cn (C. Tian).

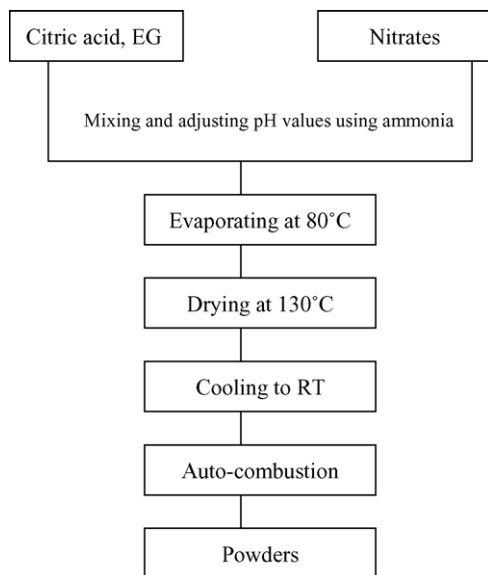


Fig. 1. Flow chart for preparing  $\text{Ni}_1\text{Co}_{0.2}\text{MnO}_4$  powders by gel auto-combustion process.

which are named Sample (A). For the sake of comparison, NTC ceramics specimens with the composition of  $\text{Ni}_1\text{Co}_{0.2}\text{Mn}_{1.8}\text{O}_4$  were prepared according to the traditional solid method, using  $\text{MnCO}_3$ ,  $\text{Co}_2\text{O}_3$ ,  $\text{NiO}$  as raw materials. Compact bodies could be obtained by traditional solid method, which are named Sample (B). The microstructures of Sample (A) and Sample (B) were investigated by using scanning electron microscope (HITACHI S-570 SEM). The densities of Sample (A) and Sample (B) were measured by Archimedes method. The electric resistivities of Sample (A) and Sample (B) were measured, and the constants  $B$  were calculated by using the formula:

$$B = \frac{298.15 \times 355.15}{355.150 - 298.15} \log \frac{R_{25}}{R_{85}}$$

### 3. Results and discussion

#### 3.1. Formation of the stable sol–gel

Fig. 2 shows the XRD patterns of the dried gels prepared under different conditions. Patterns (a)–(c) are related to the dried gels prepared from the solutions, which included nitrates, citric acid but no EG. It can be inferred that the dried gels include amorphous powder,  $\text{NH}_4\text{NO}_3$  and citrate. It means that the sol–gel was unstable. Curves (d)–(g) show the XRD patterns of dried gels prepared from the solutions, which included nitrates, citric acid and EG. We can see that the dried gels include amorphous powder and  $\text{NH}_4\text{NO}_3$ ; no crystalline phase related to metal cations appeared in the dried gels obtained at pH 3–6. The dried gels related to patterns (g) include traces of  $\text{NH}_4\text{NO}_3$ . It means that  $\text{NH}_4^+$  and  $\text{NO}_3^-$  were dispersed in the gel network. With the increase of pH values, the gel network could not contain more  $\text{NH}_4\text{NO}_3$ , superfluous  $\text{NH}_4\text{NO}_3$  separated out of the network.

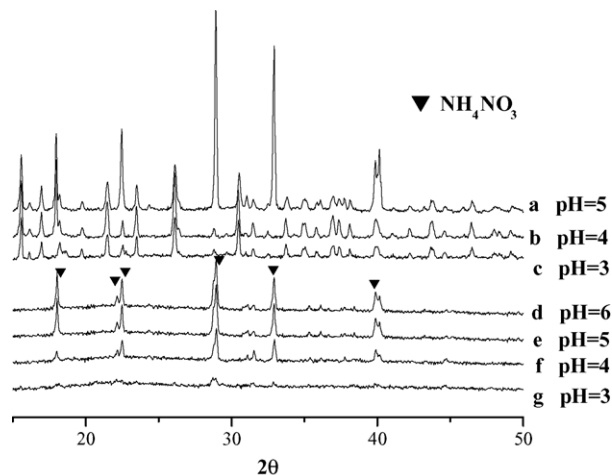


Fig. 2. XRD patterns of dried gels obtained at different conditions. The dried gels related to (a–c) were prepared from the solutions without addition of EG. The dried gels related to (d–g) were prepared from the solutions with addition of EG.

All gels discussed below were prepared from the solution at pH 3 with the addition of EG.

#### 3.2. Reaction mechanism

##### 3.2.1. The combustion and decomposition of the gels

Fig. 3 shows the DSC curve as well as the TG plot of the dried gel. It can be deduced that the combustion process of the dried gel can be divided into two steps. The first step is the decomposition and the auto-combustion of gel. The combustion and decomposition take place at about 200 °C. The second step is combustion and decomposition of remnant carboxylate at about 290 °C. Above 300 °C, the weight of sample kept unchanged.

##### 3.2.2. The formation of spinel phase

Curve (a) in Fig. 4 shows the XRD pattern of as-burnt powder. The curves (b)–(g) show the XRD patterns of

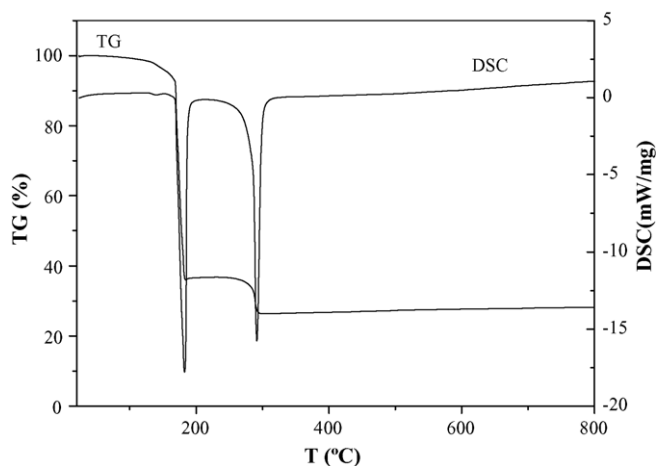


Fig. 3. The DSC and TG curves of the dried gel.

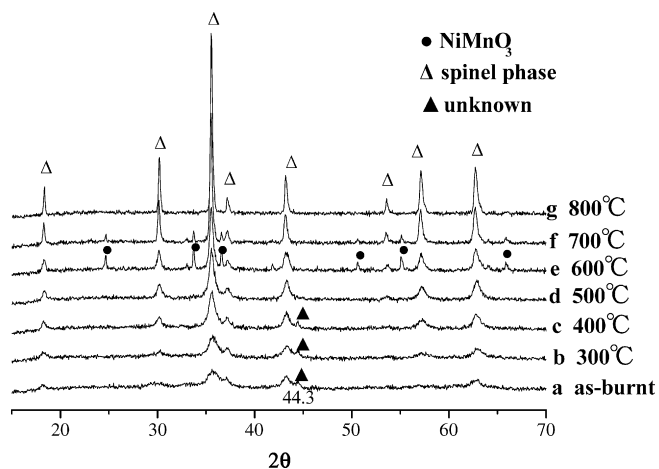


Fig. 4. XRD patterns of the as-burnt powder and the as-calcined powders at indicated temperature.

as-calcined powders heated in the furnace at various temperatures (300, 400, 500, 600, 700 and 800 °C).

The XRD patterns of powders calcined at 300 and 400 °C were similar with curve (a) in Fig. 4, in which most peaks are attributed to the spinel-type structure. We should pay more attention on the XRD peak centered at 44.3 in  $2\theta$ . In our study, we cannot identify the peak of 44.3 in  $2\theta$ , which may be attributed to the trace of remnant carboxylate. The XRD pattern of as-calcined powder at 500 °C shows that the XRD peak centered at 44.3 in  $2\theta$  has disappeared, which means that all decomposition was accomplished, and that the single spinel phase formed partly.

Diagram (e) in Fig. 4 shows the XRD pattern of as-calcined powder heated at 600 °C. A new phase,  $\text{NiMnO}_3$ , has formed. The formation of  $\text{NiMnO}_3$  phase may be related to the decomposition of the remnant carboxylate. It is plausible that the metal oxides formed in the different steps have dissimilar reactive activities. The diagrams (f) and (g) show that the content of  $\text{NiMnO}_3$  decreases after being heated at 700 °C, and

eliminates after being heated at 800 °C, accompanied by the formation of the single spinel-type phase. It is suggested that  $\text{NiMnO}_3$  transform into the  $\text{NiMn}_2\text{O}_4$ . The chemical reaction equation is:



There is no XRD pattern of MnO in the Fig. 4. Therefore, it is deduced that the MnO was amorphous in the powders.

The lattice parameter ( $a$ ) values were calculated by the well known method. The ( $a$ ) values of the spinel phase synthesized at 500 and 800 °C were evaluated as the following:  $a_{500} = 0.8354$  nm and  $a_{800} = 0.8371$  nm. We believe that the enlargement of crystal cell was caused by the entrance of  $\text{Ni}^{2+}$  cation and  $\text{Mn}^{3+}$  cation.

In Fig. 3, we did not find any TG and DSC peaks between 500 and 800 °C. This means that no thermal effect in the above transition was observed in our study. According to the phase diagram of NiO and  $\text{Mn}_2\text{O}_3$ , one eutectic compound related to  $\text{NiMnO}_3$  and  $\text{NiMn}_2\text{O}_4$  can form at about 700 °C.

So, it is reasonable that the transition of  $\text{NiMnO}_3 + \text{MnO} \rightarrow \text{NiMn}_2\text{O}_4$  can easily take place at about 700 °C.

### 3.3. The sintering activity of $\text{Ni}_1\text{Co}_{0.2}\text{Mn}_{1.8}\text{O}_4$ powder

Fig. 5 gives the SEM images of Sample (A) and Sample (B).

It can be seen that the crystalline grains in SEM photograph (a) are perfect to the crystalline grains in SEM photograph (b). The densities of samples were measured as follows: the degree of densification of Sample (A) is 97%, while the degree of densification of Sample (B) is 94%. The electrical characters of Sample (A) were measured as follows: the  $\rho(25) = 2$  k $\Omega$  cm,  $B = 3600$  K, while the electrical characters of Sample (B) were measured as follows: the  $\rho(25) = 2.3$  k $\Omega$  cm,  $B = 3350$  K. The electrical characters are accordant to the microstructures.

All of these demonstrate that the powders synthesized by the gel auto-combustion process have a high sintering activity.

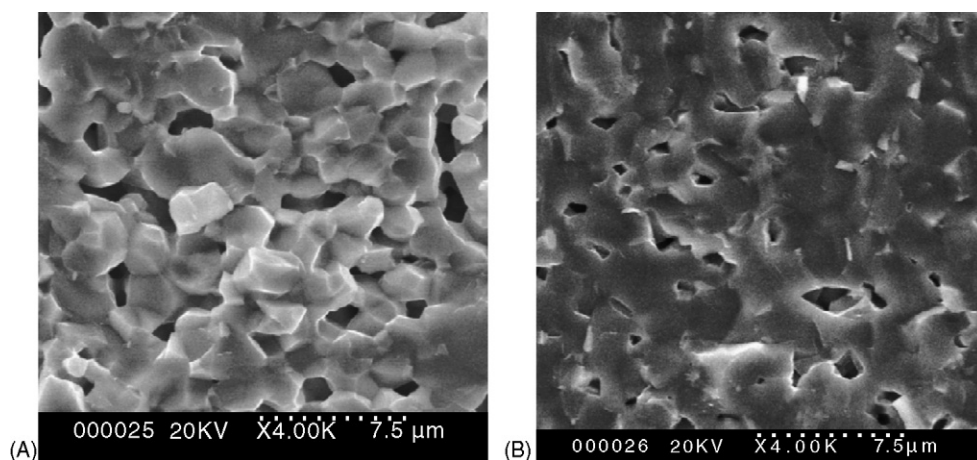


Fig. 5. SEM images Sample (A) and Sample (B).

## Acknowledgement

This work was supported by CHINA Aviation Found (02G53044).

## References

- [1] P. Duran, J. Tartaj, F. Rubio, C. Moure, O. Pena, Preparation and powder characterization of spinel-type  $\text{Co}_x\text{NiMn}_{2-x}\text{O}_4$  ( $0.2 \leq x \leq 1.2$ ) by the ethylene glycol–metal nitrate polymerized complex process, *J. Eur. Ceram. Soc.* 24 (2004) 3035–3042.
- [2] J.L. Martin De Vidales, P. Garcia-Chain, R.M. Rojas, Preparation and characterization of spinel-type Mn–Co–Ni–O negative temperature coefficient ceramic thermistors, *J. Mater. Sci.* 33 (1998) 1491–1496.
- [3] Z. Yue, W. Guo, J. Zhou, Z. Gui, L. Li, Synthesis of nanocrystalline ferrites by sol–gel combustion process: the influence of pH value of solution, *J. Magn. Magn. Mater.* 270 (2004) 216–223.